Prediction Capability of Optical Coherence Tomography for Blood Glucose Concentration Monitoring

Roman V. Kuranov, Ph.D., Veronika V. Sapozhnikova, Ph.D., Donald S. Prough, M.D., Inga Cicenaite, M.D., and Rinat O. Esenaliev, Ph.D.

Abstract

Background:

Optical coherence tomography (OCT) has been shown to be a promising optical approach to noninvasive monitoring of blood glucose concentration because of its capability of probing optical properties at different depths in tissue with high resolution. This article investigates the capability of OCT to predict changes in blood glucose concentration.

Methods:

We varied blood glucose concentration in the physiological range in three sets of experiments. In the first set, we investigated large variations of blood glucose concentration ($\approx$400 mg/dl) and used 2100 OCT A scans for signal averaging. In the second set, we varied blood glucose concentration by approximately 200 mg/dl and used 8400 A scans for signal averaging. In the third set, we improved OCT blood glucose monitoring by increasing and controlling skin temperature under the OCT probe. In this set of experiments we increased the glucose concentration by approximately 300 mg/dl and used 4200 A scans for averaging.

Results:

The predicted glucose concentrations in the first two sets were lower than actual glucose concentration by 10–20% (the mean shift), while the heating and temperature control in the third set of experiments reduced the mean shift down to 1.5%. Therefore, the mean shift was reduced substantially by tissue heating and temperature control. However, it did not depend on the number of A scans to be averaged. In contrast, the uncertainty in OCT prediction of glucose concentration (the standard deviation) did not depend on heating and temperature control, but was reduced substantially from 56 to 24 mg/dl by increasing the number of A scans from 2100 to 8400, respectively.

Conclusion:

These results suggest that the accuracy of OCT-based glucose monitoring is approaching that of standard invasive and minimally invasive techniques.

J Diabetes Sci Technol 2007;1(4):470-477

Author Affiliation: University of Texas Medical Branch, Galveston, Texas

Abbreviations: optical coherence tomography (OCT)

Corresponding Author: Rinat O. Esenaliev, Ph.D., University of Texas Medical Branch, 301 University Blvd., Rt. 0456, Galveston, TX 77555-0456; email address *riesenal@utmb.edu*

Introduction

Continuous blood glucose monitoring coupled with tight glucose control significantly decreases complications and mortality in diabetic and critically ill patients.[1–3] Noninvasive methods may provide continuous, painless blood glucose monitoring and facilitate tight blood glucose control in these patients. Therefore, there is a vital need for development of a noninvasive continuous blood glucose monitoring technique. Various optical methods proposed for noninvasive glucose monitoring include near-infrared spectroscopy, mid-infrared spectroscopy, Raman spectroscopy, polarimetry, and fluorescence.[4–10] Although these techniques are promising, they require further development to provide clinically acceptable accuracy, specificity, and reproducibility. Optical coherence tomography (OCT) was proposed previously for blood glucose monitoring and was tested *in vivo*[11–13] and *in vitro*.[14,15] It was shown that OCT is capable of detecting changes in blood glucose concentration as small as a clinically acceptable value of 20 mg/dl.[12,13] We demonstrated *in vitro* that glucose-induced changes in the OCT signal were 10-fold greater than those produced by the same changes in NaCl concentrations (major blood osmolyte).[14] Subsequent *in vivo* studies on animal model (pigs) showed 2.3-fold greater sensitivity (changes in OCT signal slope in percent per 1 mM changes in concentration of analytes) of OCT for blood glucose changes compared to OCT sensitivity to changes in Na$^+$ concentration due to NaCl injections.[16] In normal conditions, diurnal variations in Na$^+$ concentration usually does not exceed 1 mM,[17] while clinically important variations in blood glucose concentration would exceed 2 mM (36 mg/dl). Therefore, we conclude that the influence of glucose on the OCT signal slope is at least 5-fold greater than that of Na$^+$ at normal conditions. Moreover, we demonstrated that fluctuations of other biochemical and physiological variables did not produce noticeable changes in the OCT signal.[16,18]

Further development of the OCT-based glucose sensor requires testing the prediction capability of this technique in an animal model. The aim of this study was to investigate in a preclinical animal model the reproducibility of OCT blood glucose monitoring across a clinically relevant range of blood glucose concentrations and to identify major variables that influence mean shift and contribute to the uncertainty of OCT glucose monitoring.

Materials and Method

In our experiments we used a portable OCT system made in the Institute of Applied Physics of the Russian Academy of Sciences with a central wavelength of 1300 nm, a longitudinal resolution of 13 μm, and a transverse resolution of 10 μm. A detailed description of the OCT system is given elsewhere.[11,19]

In this study we acquired OCT images (300 × 400 pixels) by scanning the probing beam laterally over a 650 × 650-μm^2 area (two-dimensional lateral scanning mode).[13] Lateral scanning was performed at frequencies of approximately 12 and 0.2 Hz by two independent generators. Slow lateral scanning along a straight line was performed with an internal generator (each new lateral position corresponds to a new A scan), whereas fast scanning along a sinusoidal line was performed with the Tektronix CFG280 Function Generator (Tektronix Inc., Beaverton, OR). The OCT signal was obtained by averaging all of the 300 longitudinal scans (A scans). In turn, each longitudinal A scan on the OCT image was obtained by averaging the following numbers of individual A scans: 7, 14, and 28 in the first, second, and third sets of experiments, respectively. OCT signal slopes were obtained by a least-square linear fit of a 75-μm segment of the OCT signal. We calculated OCT signal slopes with an in-depth increment of 25 μm over the whole signal. The detailed description of acquiring and processing OCT images for calculating the OCT signal slope and the correlation coefficient between OCT signal slopes and blood glucose concentration can be found elsewhere.[13,16] To examine the prediction capability of OCT for each animal we used a segment in which we observed the maximum correlation of the OCT signal slope with glucose. The depth of this segment was different for each animal and varied in the range of 200–450 μm.

We performed three sets of experiments to study: (1) The mean shift between actual and predicted blood glucose concentrations after calibration of the OCT system using standard invasive measurements and (2) uncertainty of the predicted blood glucose concentrations. The study was conducted in 15 female pigs (weight: 20–24 kg; age: 3–4 months). Fourteen pigs were divided into three groups: 5 animals in the first set of experiments, 5 in the second set, and 4 in the third set. One pig was used as a control with no glucose administration.

Prior to the experiments the animals were anesthetized with 1% isoflurane. To prevent dehydration caused by anesthesia, the saline solution (0.9%) was slowly injected intravenously during the experiment. In the supine position, the abdominal areas (50×50 mm^2) of the pigs were shaved and then dead cells on the skin surface were removed by adhesive tape. The OCT probe was placed on the abdominal area, and OCT images were taken continuously during the whole experiment. A thin layer (thinner than the 13-μm axial resolution of the OCT system) of transparent silicon grease was used to decrease mismatch between the refractive indices of pig skin and the transparent plastic window of the OCT probe. Prior to glucose injection, OCT images were obtained for 30 min for baseline measurements. We injected glucose (50% dextrose, Abbott Laboratories, North Chicago, IL) through the femoral vein for 30 min for calibration of the OCT system (the calibration peak). One hour after the first glucose injection, another glucose peak (the prediction peak) was induced by an additional 30-min injection to study the prediction capability of the OCT system. The rate of the glucose injection for the first and third sets of experiments was 1.6 ml/min for the first 15 min followed by 4 ml/min for the last 15 min for both glucose peaks. For the second set of experiments the rate was (in both cycles) 0.4 ml/min for the first 15 min followed by 0.8 ml/min for the last 15 min. In the first two sets of experiments, we did not control the skin surface temperature of the pigs, whereas in the third set we maintained the skin surface temperature at $41.0 \pm 0.4°C$. The initial skin temperature in the first two sets of experiments was in the range of 32–33°C. At the end of the 3.5- to 4-h glucose monitoring experiment (time needed for intravenous line preparation is not included), the skin temperature under the OCT probe increased by 1–2°C. We attributed the slight increase of the temperature to a thermal isolation of skin by the OCT probe.

To calibrate the OCT system we measured glucose levels with invasive glucose meter I-STAT1 (i-STAT Corporation, East Windsor, NJ) each 5–10 min and plotted changes of OCT signal slope from baseline (ΔS_{OCT1}) versus glucose concentration (Glu_1). Then we calculated a least-square linear fit $\Delta S_{OCT1} = \kappa\, Glu_1 + b1$, where κ is a regression coefficient and b1 is the hypothetical change of OCT signal slope from the baseline glucose concentration to zero. Using OCT signal slopes measured during the second peak (S_{OCT2}) and the calculated regression coefficient κ, we predicted glucose concentrations (Glu_{pred}) during the second peak $Glu_{pred} = (\Delta S_{OCT2} - b1)/\kappa$. These predicted values of glucose concentration were compared with those measured by I-STAT1 during the second glucose peak. The I-STAT1 device allowed simultaneous measurement in one EC8+ cartridge of glucose and other major analytes, such as Na, K, CL, pH, PCO_2, blood urea nitrogen/urea, and hematocrit, and permitted assessment of their influence on calibration and prediction.

In the first set we used a large variation of blood glucose concentration and a low number (2100) of A scans for signal averaging. Acquisition time for a single OCT image was 30 s. We increased the blood glucose concentration from baseline 72 ± 20 to 470 ± 90 mg/dl in the calibration peak and from 158 ± 24 to 480 ± 60 mg/dl in the prediction peak. The first numbers correspond to the mean baseline glucose concentration for all five pigs used in the first set of experiments, whereas the second numbers are the standard deviation between baseline concentrations in these five pigs. Blood glucose concentration decreased after the glucose injection as a consequence of pig physiology (no injection of insulin was performed).

In the second set, we varied blood glucose concentrations in the lower range: from 72 ± 20 to 210 ± 24 mg/dl in the calibration peak and from 84 ± 12 to 232 ± 15 mg/dl in the prediction peak. The number of averaged A scans was 8400, resulting in an acquisition time of 2 min for a single OCT image.

In the third set, blood glucose concentrations were varied in the range from 93 ± 13 to 417 ± 6 mg/dl in the calibration peak and from 146 ± 23 to 395 ± 20 mg/dl in the prediction peak. The number of averaged A scans was 4200 at an acquisition time of 1 min for a single OCT image.

Results

In all 14 animals the correlation between OCT signal slope and changes in blood glucose concentration was high: $|R| > 0.8$ (absolute value of correlation coefficient), $p < 0.01$ for the prediction peak and $|R| > 0.7$, $p < 0.01$ for both peaks. As expected,[13] a maximal correlation was detected at the derma–hypoderma and papillary–reticular junctions.

Raw data on the OCT signal slope and blood glucose concentrations for each set of experiments are presented in **Figure 1**. **Figures 1a** (the first set of experiments) and **1b** (the second set of experiments) show that variation of the actual blood glucose concentration induces fewer changes in the OCT signal slopes in the second peak compared to those in the first peak.

For example, in the first set of experiments (**Figure 1a**), a variation in blood glucose concentration of 460 mg/dl changed the OCT signal slope by 44% (0.95% per 10 mg/dl) for the calibration peak, whereas a variation of 330 mg/dl changed the OCT slope by 26% (0.79% per 10 mg/dl) for the prediction peak. In the second set of experiments (**Figure 1b**), a variation in blood glucose concentration of 150 mg/dl changed the OCT signal slope by 42% (2.80% per 10 mg/dl) for the calibration peak, whereas a variation of 145 mg/dl changed the OCT slope by 26% (1.78% per 10 mg/dl) for the prediction peak. In contrast, in the third set of experiments with temperature control, changes in OCT signal slopes in the first and second peaks were very close (**Figure 1c**). In **Figure 1c** (third set of experiments), a variation in blood glucose concentration of 325 mg/dl changed the OCT signal slope by 38% (1.17% per 10 mg/dl) for the calibration peak, whereas a variation of 250 mg/dl changed the OCT slope by 28% (1.13% per 10 mg/dl) for the prediction peak. The correlation of the OCT signal slope with blood glucose concentration was much better when skin heating and temperature control were used. These improvements in correlation were associated with an increase of skin microcirculation and glucose diffusion in the tissue at higher temperatures.[20] Averaging of independent A scans did not influence the correlation of OCT with blood glucose concentration.

To calculate the mean shift and uncertainty in the prediction peak, we first plotted changes in the OCT signal slope vs blood glucose concentration for the calibration peak. **Figures 2a**, **3a**, and **4a** show this dependence for the three sets of experiments, respectively. The influence of the motion artifacts and temperature instability may result in a significant deviation of OCT signal slope from linear dependence on blood glucose concentration (see, for instance, change in OCT signal slope at a glucose concentration of 160 mg/dl in **Figure 2a**). We then plotted the difference between OCT predicted and actual blood glucose concentrations for the prediction peak (**Figures 2b**, **3b**, and **4b**). Data indicate that, on average, the predicted glucose concentrations in the first two sets of experiments (**Figures 2b** and **3b**) were lower than the actual glucose concentrations by 10–20%, i.e., the mean shift = 10–20%. The local skin heating and temperature control reduced the mean shift down to 1.5% in the third set of experiments (**Figure 4b**). The mean shift did not depend on the number of averaged A scans.

The uncertainty in OCT prediction of glucose concentration (the standard deviation) did not depend on the heating and temperature control, but was reduced substantially from ±56 to ±24 mg/dl by
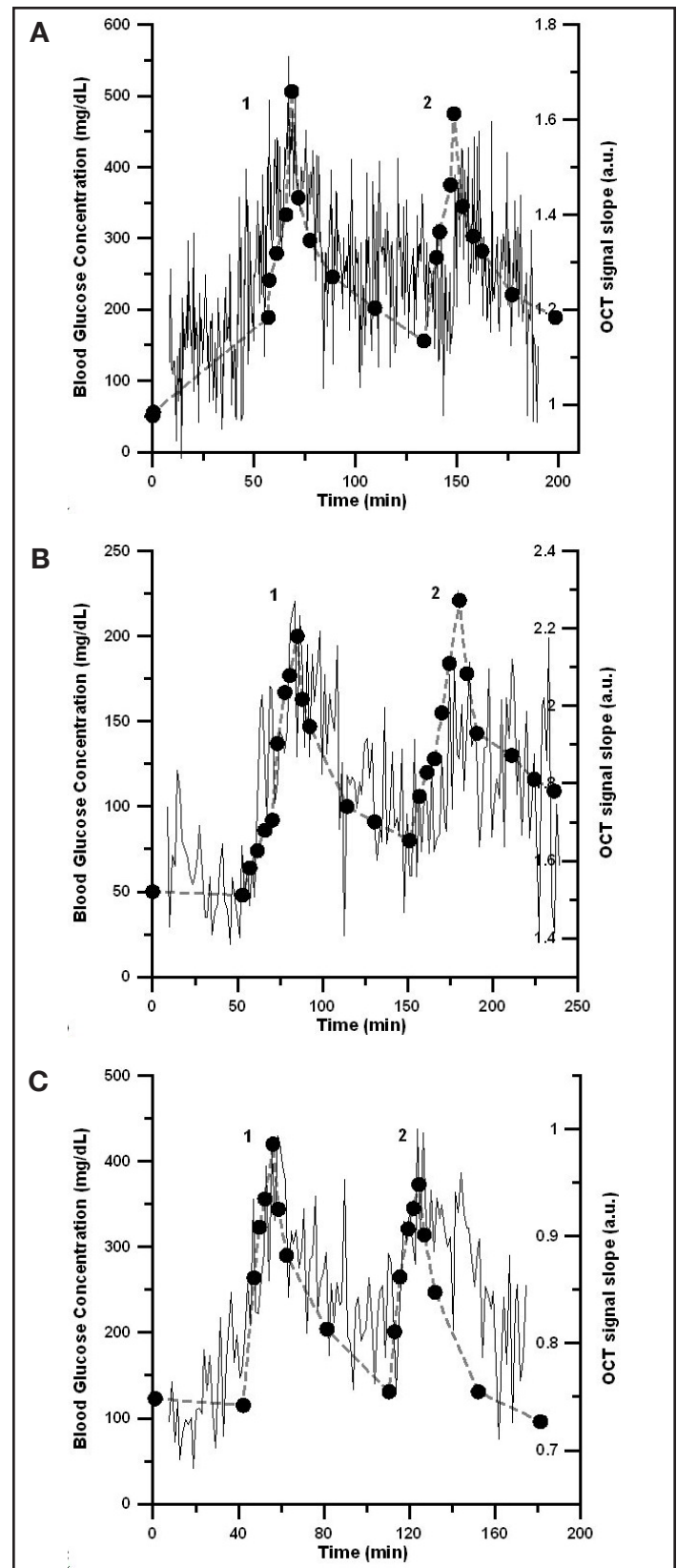

Figure 1. Typical OCT signal slopes (solid lines) and corresponding actual blood glucose concentrations (circles connected with dashed lines) measured in (**A**) the first set of experiments, (**B**) the second set of experiments, and (**C**) the third set of experiments. The first peak was used for calibration of the OCT system, and the second peak was used for prediction of blood glucose concentration.
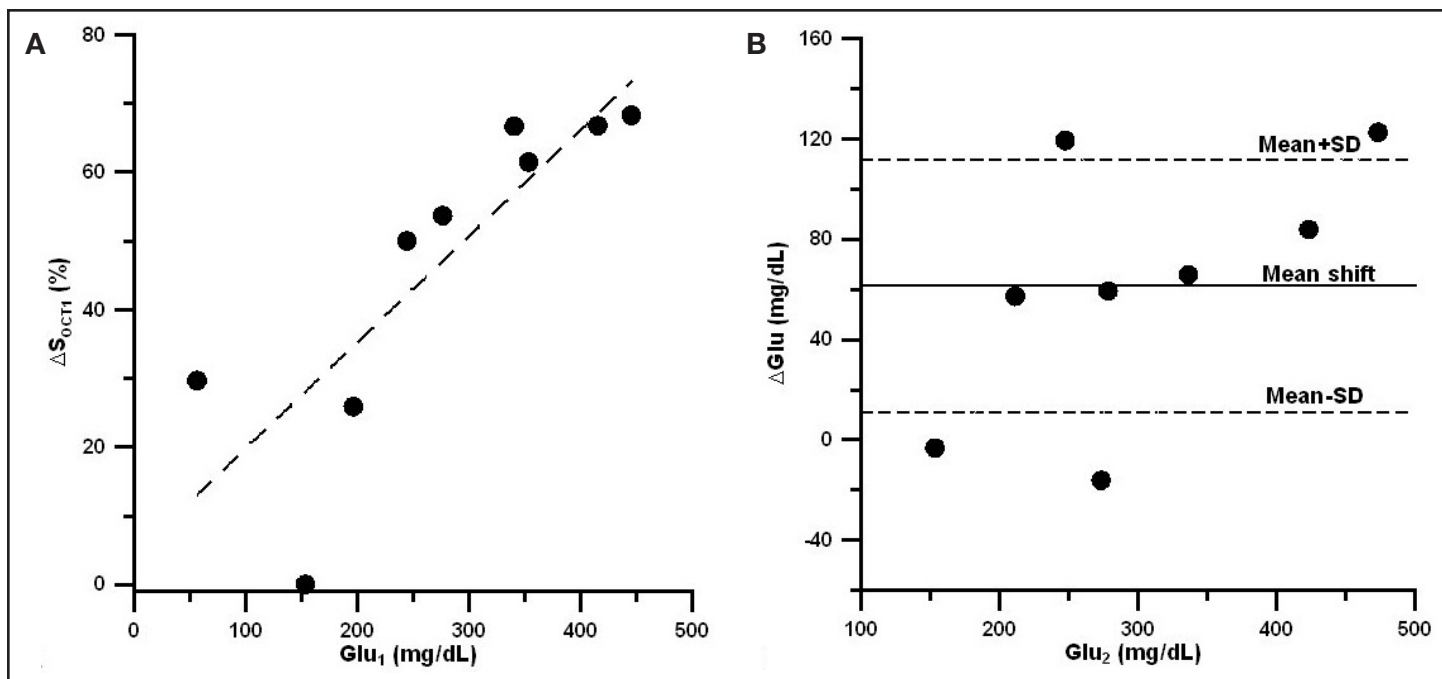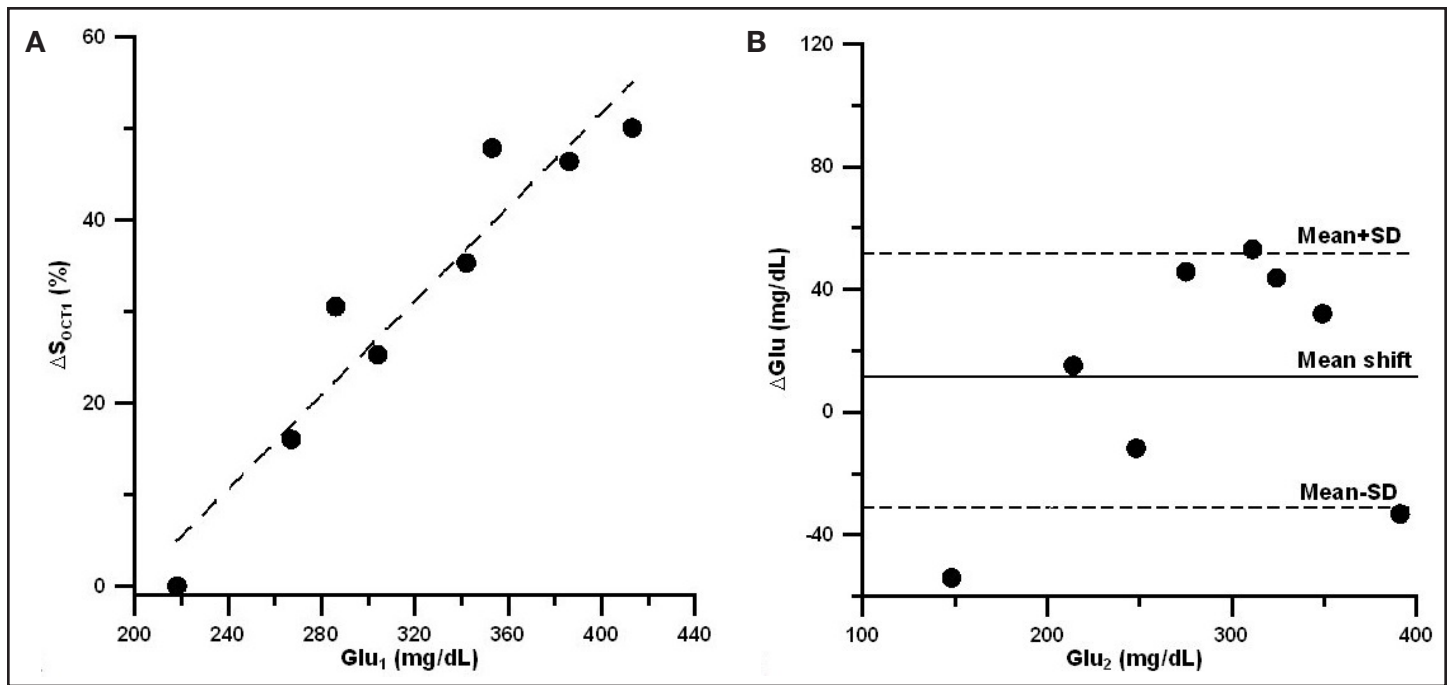
Figure 2. (**A**) Typical relative OCT signal slope changes from baseline (ΔS_{OCT1}) vs actual blood glucose concentration (Glu_1) measured during the calibration peak for the first set of experiments. The dashed line is the linear regression. (**B**) Typical difference (ΔGlu) between actual blood glucose concentration (Glu_2) and predicted glucose concentration (Glu_{pred}) vs actual glucose concentration during the second peak for the first set of experiments. The solid line represents the mean shift in blood glucose prediction with OCT (the predicted values of glucose concentration were always less than the actual ones), and dashed lines represent mean shift + standard deviation (SD) and mean shift – SD in prediction of blood glucose concentration.
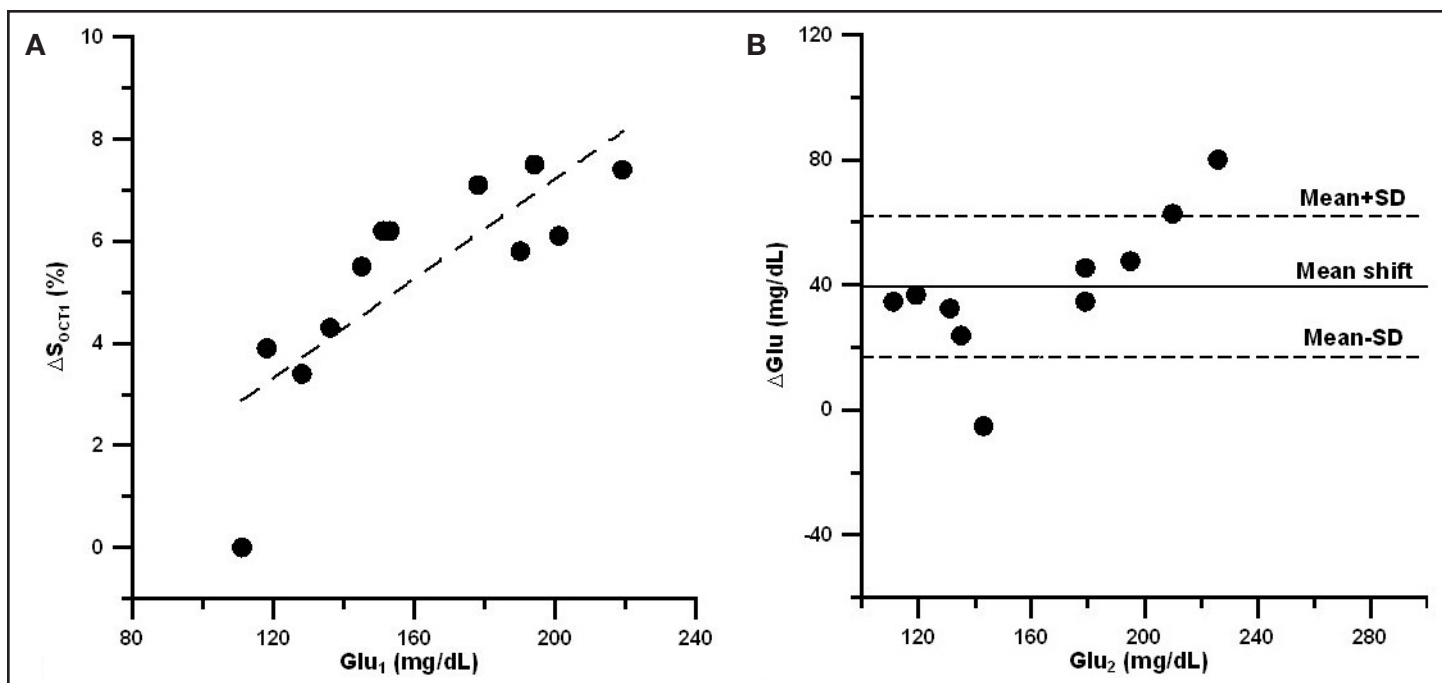
Figure 3. (**A**) Typical relative OCT signal slope changes from baseline (ΔS_{OCT1}) vs actual blood glucose concentration (Glu_1) measured during the calibration peak in the second set of experiments. (**B**) Typical difference (ΔGlu) between actual blood glucose concentration (Glu_2) and predicted glucose concentration (Glu_{pred}) vs actual glucose concentration during the second peak for the second set of experiments.

Figure 4. (**A**) Typical relative OCT signal slope changes from baseline (ΔS_{OCT1}) vs actual blood glucose concentration (Glu_1) measured during the calibration peak in the third set of experiments. (**B**) Typical difference (ΔGlu) between actual blood glucose concentration (Glu_2) and predicted glucose concentration (Glu_{pred}) vs actual glucose concentration during the second peak for the third set of experiments.

Table 1.
Mean Shift and Uncertainty of Prediction at Different Experimental Conditions

Parameter	First set	Second set	Third set
Mean prediction shift, mg/dl	53 ± 31	39 ± 6	4.5 ± 15
Prediction uncertainty, mg/dl	56 ± 20	24 ± 7	38 ± 7
Number of averaged A scans	2100	8400	4200
Temperature control	No	No	Yes

increasing the number of averaged A scans from 2100 to 8400, respectively. Major results on the main shift and uncertainty are summarized in **Table 1**.

Changes in the OCT signal slope did not correlate with variations of other blood analytes. The influences of other blood analytes on the capability of OCT to predict blood glucose concentration were not significant.

Discussion

Results obtained in the first two sets of experiments indicate that glucose-induced changes in the OCT signal slope in the calibration peak were significantly greater than in the prediction peak. We have proposed a likely mechanism for correlation of the OCT signal slope with blood glucose concentration based on structural tissue alterations induced by glucose osmotic effects.[13] Hence, the mean shift of 10–20% in the first set of experiments may be explained by incomplete recovery of the interstitial water content in the skin of anesthetized animals after the first glucose injection. A less mean shift in the second set can be attributed to a lower variation of blood glucose concentration compared to that in the first set of experiments.

Local skin heating increases blood perfusion and other metabolic processes in skin.[20] Therefore, to accelerate skin metabolism and the recovery of skin water content, one can heat the skin probing area and maintain it at a higher temperature. Results demonstrated that skin heating and temperature control at 41.0 ± 0.4°C significantly decrease the mean shift from 53 mg/dl in the first set down to 4.5 mg/dl in the third set of experiments for similar changes in blood glucose concentration: 360 and 286 mg/dl are average changes in the two peaks for the first and

third sets of experiments, respectively. We anticipate that in humans the temperature control will substantially decrease the mean shift as well as a consequence of a similar influence of temperature-dependent effects on skin physiology.

The increase of the number of A scans to be averaged from 2100 to 4200 resulted in a substantial decrease of standard deviation: from 56 to 38 mg/dl (**Table 1**). When we further increased the number of averaged A scans up to 8400, the standard deviation decreased to 24 mg/dl. The maximum number of independent A scans that can be achieved in our studies is 4225. This number was calculated by squaring the number of maximum nonoverlapping (independent) A scans for one-dimensional scanning (along the straight line), that is 65, which was obtained by dividing the scanning range (650 μm) by the probing beam diameter of 10 μm. Two thousand one hundred A scans covered about 30% of the 650×650-μm^2 scanning area (**Figure 5a**), 4200 A scans covered about 50–60% (**Figure 5b**), and 8400 A scans covered close to 100% of the scanning area (**Figure 5c**). Because of the nonlinearity of sinusoidal scanning, the packing of A scans is much greater near extrema $x_n^s = (n+1) \cdot \pi / 2$ than near zero values of sinus $x_n^f = n \cdot \pi$ ($n = 0, 1, 2, \ldots$) because the scanning near extrema is slower. Therefore, the efficacy of averaging decreased at the higher number of the averaged A scans.

Conclusion

In this work we achieved uncertainty in the prediction ability of OCT in the blood glucose concentration of 24 ± 7 mg/dl. We demonstrated that the uncertainty can be lowered significantly by increasing the number of A scans to be averaged. However, the number of averaged A scans did not influence the mean shift in the prediction of blood glucose concentration by OCT.

We also minimized the mean shift by increasing the rate of skin metabolism using local heating of the skin surface. Based on obtained data, one can conclude that the mean shift in OCT prediction after a sharp increase of blood glucose concentration in anesthetized animals is most likely caused by an incomplete recovery of water content skin dehydrated due to a high blood glucose concentration produced in the calibration peak. One can anticipate that in nonanesthetized diabetic and nondiabetic patients the mean shift will be even less.
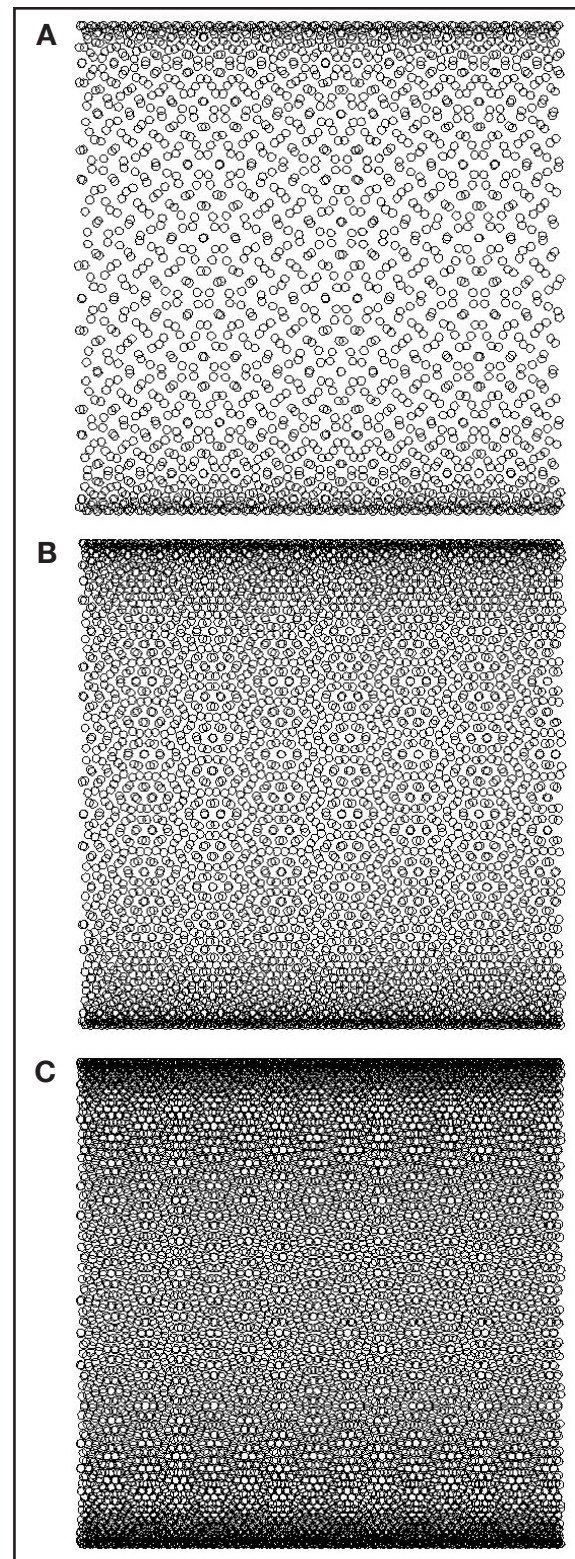
Figure 5. (**A**) Infilling of the scanned area of pig skin with probing OCT beam during two-dimensional scanning mode in the first set of experiments. (**B**) Infilling for the third set of experiments. (**C**) Infilling for the second set of experiments. Calculations were performed with the following parameters: scanning area, 650 x 650 μm^2; OCT beam diameter, 10 μm. A fast sinusoidal scan was performed along the y axis with a frequency of 11.99 Hz. A slow linear scan was performed along the x axis with a frequency of 0.2 Hz. The number of averaged A scans was 2100, 4200, and 8400 for **A**, **B**, and **C**, respectively.

References:

1. The Diabetes Control and Complications Trial Research Group. The effect of intensive treatment of diabetes on the development and progression of long-term complications in insulin-dependent diabetes mellitus. N Engl J Med. 1993 Sep 30;329(14):977-86.

2. Wild S, Roglic G, Sicree R, Green A, King H. Global burden of diabetes mellitus in the year 2000. In: Global Burgen of Disease 2000. Geneva: World Health Organization; 2003.

3. van den Berghe G, Wouters P, Weekers F, Verwaest C, Bruyninckx F, Schetz M, Vlasselaers D, Ferdinande P, Lauwers P, Bouillon R. Intensive insulin therapy in the critically ill patients. N Engl J Med. 2001 Nov 8;345(19):1359-67.

4. Olesberg JT, Liu L, Van Zee V, Arnold MA. *In vivo* near-infrared spectroscopy of rat skin tissue with varying blood glucose levels. Anal Chem. 2006 Jan 1;78(1):215-23.

5. Enejder AM, Scecina TG, Oh J, Hunter M, Shih WC, Sasic S, Horowitz GL, Feld MS. Raman spectroscopy for noninvasive glucose measurements. J Biomed Opt. 2005 May-Jun;10(3):031114.

6. Wan Q, Coté GL, Dixon JB. Dual-wavelength polarimetry for monitoring glucose in the presence of varying birefringence. J Biomed Opt. 2005 Mar-Apr;10(2):024029.

7. Klonoff DC. Continuous glucose monitoring: roadmap for 21st century diabetes therapy. Diabetes Care. 2005 May;28(5):1231-9.

8. Klonoff DC. Noninvasive blood glucose monitoring. Diabetes Care. 1997 Mar;20(3):433-7.

9. McNichols RJ, Coté GL. Optical glucose sensing in biological fluids: an overview. J Biomed Opt. 2000 Jan;5(1):5-16.

10. Khalil OS. Non-invasive glucose measurement technologies: an update from 1999 to the dawn of the new millennium. Diabetes Technol Ther. 2004 Oct;6(5):660-97.

11. Esenaliev R, Larin K, Larina I, Motamedi M. Noninvasive monitoring of glucose concentration with optical coherence tomography. Opt Lett. 2001;26:992-4.

12. Kuranov R, Prough D, Sapozhnikova V, Cicenaite I, Esenaliev R. *In vivo* application of 2-D lateral scanning mode optical coherence tomography for glucose sensing. In: Cullum BM, Carter J, editors. Smart medical and biomedical sensor technology III. Proc. SPIE; V. 6007; 2005. p. 90-95.

13. Kuranov RV, Sapozhnikova VV, Prough DS, Cicenaite I, Esenaliev RO. *In vivo* study of glucose-induced changes in skin properties assessed with optical coherence tomography. Phys Med Biol. 2006 Aug 21;51(16):3885-900.

14. Larin KV, Akkin T, Esenaliev RO, Motamedi M, Milner TE. Phase-sensitive optical low-coherence reflectometry for the detection of analyte concentration. Appl Opt. 2004 Jun 10;43(17):3408-14.

15. Kinnunen M, Myllylä R, Jokela T, Vainio S. *In vitro* studies toward noninvasive glucose monitoring with optical coherence tomography. Appl Opt. 2006 Apr 1;45(10):2251-60.

16. Sapozhnikova VV, Prough D, Kuranov RV, Cicenaite I, Esenaliev RO. Influence of osmolytes on *in vivo* glucose monitoring using optical coherence tomography. Exp Biol Med (Maywood). 2006 Sep;231(8):1323-32.

17. Guyton AC. Textbook of medical physiology. Phildelphia: W. B. Saunders; 1981. p. 435-443.

18. Larin KV, Motamedi M, Ashitkov TV, Esenaliev RO. Specificity of noninvasive blood glucose sensing using optical coherence tomography technique: a pilot study. Phys Med Biol. 2003 May 21;48(10):1371-90.

19. Kholodnykh AI, Petrova IY, Larin KV, Motamedi M, Esenaliev RO. Precision of measurement of tissue optical properties with optical coherence tomography. Appl Opt. 2003 Jun 1;42(16):3027-37.

20. Lokshina AM, Song CW, Rhee JG, Levitt SH. Effect of fractionated heating on the blood flow in normal tissues. Int J Hyperthermia. 1985 Apr-Jun;1(2):117-29.